Solar Energy Materials & Solar Cells 226 (2021) 111085

Contents lists available at ScienceDirect

Solar Energy Materials and Solar Cells

journal homepage: http://www.elsevier.com/locate/solmat

New insights on LeTID/BO-LID in p-type mono-crystalline silicon

Dehang Lin [a], Zechen Hu [a], Qiyuan He [a], Deren Yang [a], Lihui Song [a,b,**], Xuegong Yu [a,*]

[a] State Key Laboratory of Silicon Materials and Department of Materials Science and Engineering, Zhejiang University, No.38 Zheda Road, Hangzhou, 310027, China
[b] College of Materials & Environmental Engineering, Hangzhou Dianzi University, No. 1 nd Street Jianggan District, Hangzhou, 310018, China

ARTICLE INFO

Keywords:
LeTID
Boron-oxygen defects
Mono-crystalline silicon
Degradation
Hydrogen

ABSTRACT

In this work, light-induced degradation (LID) experiments were performed on p-type boron-doped Czochralski silicon (Cz-Si) wafers under different conditions, aiming to separately characterize boron-oxygen related LID (BO-LID) and "light and elevated temperature-induced degradation" (LeTID). We found that the regeneration rate of BO-LID, as well as the extent and kinetics of LeTID, were strongly influenced by peak firing temperature. These dependences can be explained by the variation of hydrogen concentration, which was modulated by peak firing temperature. Furthermore, we found that extending the duration of dark annealing pre-treatment decelerates the subsequent regeneration of BO defects. This result revealed that, under dark annealing, the evolution of LeTID was accompanied by a notable decrease in the mobile hydrogen concentration. Supported by this phenomenon, a hydrogen-related model based on reversible reaction is proposed to describe the LeTID behavior in crystalline silicon.

1. Introduction

The passivated emitter and rear cell (PERC) technology enables current and future commercial cells with an efficiency of 21–24% at a relatively low cost [1]. However, PERC cells fabricated from boron-doped Czochralski silicon (Cz-Si) suffer from light-induced degradation (LID), due to the formation of recombination-active defects. These defects, formed under excess carrier injection by illumination or forward-biasing, can cause severe degradation in efficiency [2,3].

The activation of boron-oxygen (BO) defects is one of the most prominent cases of LID in Cz-Si, which is often denoted by "BO-LID". This degradation takes effect under carrier injection at room temperature and leads to a relative efficiency loss of up to 10%, depending on the boron and oxygen concentrations [4]. Aiming to suppress BO-LID, recent researches by Herguth et al. have shown that BO defects can be permanently deactivated by simultaneous illumination and annealing under one sun intensity at 60–200 °C [5,6], which is often referred to as a regeneration process.

In addition to BO-LID, Ramspeck et al. observed multicrystalline silicon (mc-Si) solar cells with PERC structure suffer from about 6% relative efficiency loss when illuminated at elevated temperatures above 50 °C [7]. This unexpectedly severe degradation exceeds the range that could be explained by the well-established BO-LID models or iron-boron (Fe–B) pairs dissociation [7–9]. Due to its temperature dependence, this effect was later named as light and elevated temperature-induced degradation (LeTID) [10]. Apart from mc-Si, some recent works have demonstrated that LeTID-related defects also exist in p-type Cz-Si [11,12]. Since BO-LID could be reliably eliminated, LeTID becomes much unfavorable in Cz-Si solar cells, causing a degradation of up to 4% (relative) [13].

Several methods have been proposed to quantify LeTID in p-type Cz-Si. Recently, Chen et al. manifested that LeTID can also be triggered by dark annealing above 175 °C [11]. This method has been used to evaluate LeTID in several studies [11,14,15]. Besides, Wagner et al. suggested a one-week (163 h) degradation at 75 °C could complete the BO-LID cycle and consequently enable the measurement of the LeTID strength [12]. Nevertheless, more results are still needed in order to assess and understand LeTID in Cz-Si solar cells.

In recent years, extensive studies have been published to discuss the general mechanisms of LID. Of our particular interest is the recent observation that hydrogen plays an interesting and important role in LID. On one hand, several authors noted that the LeTID only occurred on

* Corresponding author. State Key Laboratory of Silicon Materials and Department of Materials Science and Engineering, Zhejiang University, No.38 Zheda Road, Hangzhou, 310027, China.
** Corresponding author. College of Materials & Environmental Engineering, Hangzhou Dianzi University, No. 1 nd Street Jianggan District, Hangzhou, 310018, China.
E-mail addresses: lhsong@hdu.edu.cn (L. Song), yuxuegong@zju.edu.cn (X. Yu).

https://doi.org/10.1016/j.solmat.2021.111085
Received 16 December 2020; Received in revised form 24 March 2021; Accepted 25 March 2021
Available online 3 April 2021
0927-0248/

samples that were fired with a hydrogen-rich passivation layer [16] and the degradation extent increased with the peak firing temperature [17,18]. Moreover, a certain correlation between the hydrogen concentration in silicon bulk and the extent of LeTID has been observed through different approaches [19,20]. On the other hand, hydrogen can permanently deactivate BO defects, preventing BO-LID under subsequent illumination, as suggested by Wilking et al. [21,22]. Since a mass of hydrogen in the passivation layers can in-diffuse at temperatures above 500 °C [23], the firing process leads to a considerable variation in hydrogen concentration in bulk. Thus, a study on the impact of firing temperature on LID is needed, as hydrogen may alter the behaviors of both degradation paths in p-type Cz-Si.

In the first part of this work, we investigated the impact of peak firing temperature on LID in p-type Cz-Si wafers. The results showed that the regeneration process of BO-LID, as well as the extent and kinetics of LeTID, were strongly influenced by peak firing temperature. These dependences can be interpreted by the variation in hydrogen concentration. In the second part, we investigated the behaviors of LeTID during the dark annealing treatment via monitoring the subsequent regeneration kinetics of BO-LID. The results implied that, the evolution of LeTID is accompanied by a decrease in the mobile hydrogen concentration. Finally, we proposed a hydrogen-related model to explain the experimental results and give new insights on LeTID.

2. Experimental details

2.1. Sample preparation

Boron-doped Cz-Si sister wafers with a resistivity of 0.8 Ωcm, thickness of 180 μm and length of 156 mm were used in this study. The interstitial oxygen concentration was determined to be 9×10^{17} cm^{-3} by Fourier transform infrared spectrometer (FTIR) at room temperature. The lifetime samples were fabricated on a commercial production line using standard process: alkaline texturing, phosphorous diffusion (~140 Ω/sq), phosphosilicate glass removal, rear surface polishing and deposition of surface layers. An antireflection coating (75 nm SiN_x) and a passivation stack (10 nm Al_2O_3/75 nm SiN_x) were deposited on the front and rear surfaces, respectively. The Al_2O_3 film was deposited using atomic layer deposition (ALD) tool at about 260 °C. The SiN_x film with a refractive index of 2.11 at 633 nm was deposited using plasma enhanced chemical vapor deposition (PECVD) tool at about 480 °C. Then, samples were subjected to a firing process with different peak temperatures of 650–850 °C using a rapid thermal process (RTP) furnace. The firing ramp rate was set to about 50 °C/s and the cooling rate were adjusted to about 40 °C/s, in order to mimic the metallization process in commercial solar cell fabrication line. Finally, the samples were cleaved into 39 mm × 39 mm pieces to streamline the ensuing experiments.

For the experiments of BO-LID, the samples were first illuminated under 0.1 suns at 25 °C for 48 h. Then, these samples were imposed to illumination of 0.7 suns at an elevated temperature of 130 °C controlled by a hotplate. For the LeTID study, samples were annealed on a hotplate in the dark at 200 °C.

The carrier lifetime measurements were carried out using quasi-steady-state photoconductance (QSSPC) technique at 25 ± 1 °C with a fixed injection level of $\Delta n = 1.5 \times 10^{15}$ cm^{-3} [24]. The normalized defect concentration N_t was derived from the measured lifetime according to

$$N_t = \frac{1}{\tau(t)} - \frac{1}{\tau(0)} = \left(\frac{1}{\tau_{SRH}} + \frac{1}{\tau_{res}}\right) - \frac{1}{\tau_{res}} \quad (1)$$

where $\tau(t)$ is the lifetime measured at the illumination or dark annealing time t, $\tau(0)$ is the initial lifetime, τ_{SRH} and τ_{res} are the lifetime limited by the generated recombination-active bulk defects and the residual defects, respectively. Note that N_t is proportional to the generated defect concentration on the condition that no second defect is generated.

2.2. Characterization of BO-LID and LeTID

For Cz-Si solar cells under field condition, BO-LID and LeTID may occur simultaneously. In order to separate these two effects, specific conditions were used to trigger the degradation and regeneration. Fig. 1 shows the evolution of effective minority carrier lifetime for the samples after firing at 750 °C under three different conditions: (I) 25 °C, 0.1 suns; (II) 130 °C, 0.7 suns; and (III) 200 °C, dark annealing. A two-step process presented in Fig. 1(a) was applied for measuring the BO-LID behavior. The as-fired sample was first completely degraded at a relatively low temperature and light intensity (25 °C and 0.1 suns), thus preventing the LeTID-related reaction. After the BO defects were fully transformed into degraded state, equivalent to a stable lifetime, the regeneration process was carried out under 0.7 suns at 130 °C. Conversely, the degradation and regeneration under dark annealing in Fig. 1(b) were solely attributed to LeTID [11], as the BO defects remain recombination-inactive (annealed state) and cannot account for the changes in the measured lifetime [25]. Since two degradations can be distinguished, we propose that Eq. (1) could be used to derive the normalized defect concentrations of BO defects $N_{t,BO}(t)$ and LeTID-related defects $N_{t,LeTID}(t)$, respectively.

However, we noticed that condition (II) is also in the range of typical LeTID conditions, which gives uncertainty to the measured regeneration curves of BO-LID. With regard to this question, the injection-dependent lifetime spectroscopy (IDLS) curves for sample investigated at Fig. 1(a) were extracted, as presented in Fig. 2. It shows that the IDLS curve for regenerated state is almost equivalent to the initial state (as-fired), suggesting the generation of LeTID-related defects is negligible under condition (II). Therefore, we suggest that although this conflict may somewhat compromise the measurement accuracy, our main conclusions still hold true.

As in previous studies, the degradation and regeneration of BO-LID can be described respectively by the following exponential functions.

$$N_{t,BO}(t) = N_\infty\left(1 - \exp\left(-R_{deg,BO}t\right)\right) \text{ for } t \text{ in degradation} \quad (2)$$

$$N_{t,BO}(t) = N_0 \exp\left(-R_{reg,BO}t\right) \text{ for } t \text{ in regeneration} \quad (3)$$

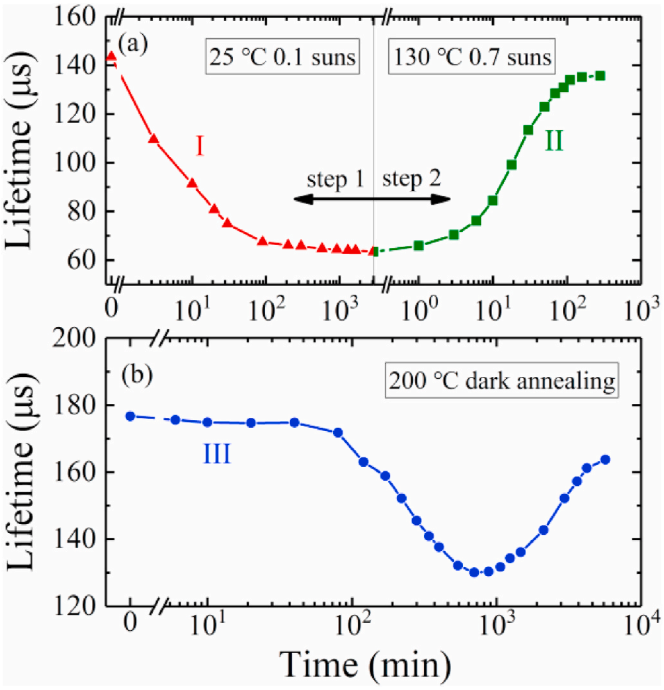

Fig. 1. The evolution of effective lifetime measured under three specific conditions: (I) 25 °C 0.1 suns, (II) 130 °C 0.7 suns and (III) 200 °C dark annealing. Different conditions were used to distinguish (a) BO-LID from (b) LeTID.

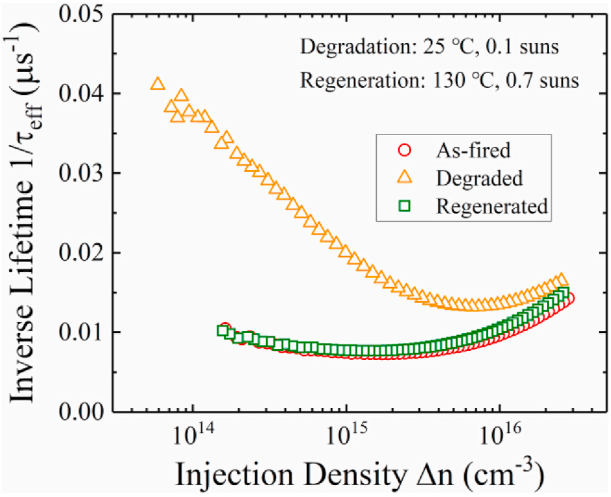

Fig. 2. IDLS curves measured at 25 °C for sample investigated in Fig. 1(a) before degradation (red), after degradation (orange) and after regeneration (green). (For interpretation of the references to colour in this figure legend, the reader is referred to the Web version of this article.)

where $R_{deg,BO}$ and $R_{reg,BO}$ are the rate constants for the degradation and regeneration processes, respectively; N_∞ and N_0 are the saturated and initial BO defect concentration, respectively.

For the kinetics of LeTID, the fact that degradation and regeneration occur simultaneously complicated its characterization. Generally, the time evolution of normalized LeTID-related defect concentration can be described with a double exponential function:

$$N_{t,LeTID}(t) = N_{max,LeTID}\left[\exp\left(-R_{deg,LeTID}t\right) - \exp\left(-R_{reg,LeTID}t\right)\right] \quad (4)$$

where $N_{max,\ LeTID}$ is the maximum possible defect concentration, $R_{deg,\ LeTID}$ and $R_{reg,\ LeTID}$ are the rate constants for the degradation and regeneration processes, respectively. It should be noted that this function is simplified to effectively extract rate constants from measured LeTID curves, and more details will be discussed in Section 4.2.

We would also like to clarify the terminology used in context. The terms "degradation" and "regeneration" refer to the reactions that lead to the increase and decrease in normalized defect concentration, respectively. For the BO-LID, the term "regeneration" is explicitly related to a specific BO defects transition, that is, from degraded state to regenerated state. However, this term does not necessarily have the same meaning in LeTID study, and we used it to simply indicate the disappearance of the recombination-active LeTID-related defects.

Moreover, the surface saturation current density J_0 was extracted at $\Delta n = 1 \times 10^{16}$ cm^{-3} to monitor the change of surface passivation quality. For samples used for lifetime measurement, the initial J_0 values were in the range of 45 ± 10 fA cm^{-2}, and the variation of J_0 during the measurement was less than 5% whether illuminated or dark-annealed. Thus, we suggest that the measured effective lifetime evolution is mainly caused by the changes of bulk lifetime.

In the following part, we will use these conditions as standard methods to characterize BO-LID and LeTID separately.

3. Results

3.1. The impact of peak firing temperature on BO-LID and LeTID

Fig. 3(a) shows the evolution of normalized BO defect concentration during a two-step process, in which we measured the degradation and regeneration of BO-LID separately. For all samples, whether fired or not, we found that the BO defects rapidly generated in the first 5 h and reached saturated concentration in 48 h (not shown). Afterwards, the time scales of regeneration in different samples vary considerably from minutes to hours, depending on the peak firing temperature. However, the unfired sample showed no increase in lifetime under the regeneration condition and thus remained in degraded state. Furthermore, the rate constants $R_{deg,BO}$ and $R_{reg,BO}$ are fitted using Eqs. (2) and (3), with the results plotted versus peak firing temperature in Fig. 3(b). As can be seen, increasing the peak firing temperature from 650 °C to 850 °C results in an increase of $R_{reg,BO}$ by a factor of 20, whereas $R_{deg,BO}$ is independent of it. According to previous studies, the regeneration rate can be sped up by higher hydrogen concentration [21,26,27]. Thus, we conclude that a higher firing temperature leads to a larger hydrogen concentration in silicon bulk and consequently deactivate BO defects more efficiently.

Fig. 4(a) presents the normalized LeTID-related defect concentration as a function of dark annealing time for samples fired at peak temperatures varying from 650 °C to 850 °C. Clearly, samples subjected to a firing process show an initial increase and a subsequent reduce of LeTID-related defects, while the unfired sample shows negligible changes during annealing. One remarkable behavior is that the degradation extent increases with the augmentation of peak firing temperature, which is consistent with previous researches on Cz-Si and mc-Si [17,18]. By fitting the curves using Eq. (4), we can further obtain the correlation of rate constants $R_{deg,\ LeTID}$ and $R_{reg,\ LeTID}$ with the peak firing temperature, as presented in Fig. 4(b). It shows that $R_{deg,\ LeTID}$ significantly increases with the augmentation of peak firing temperature, while $R_{reg,}$

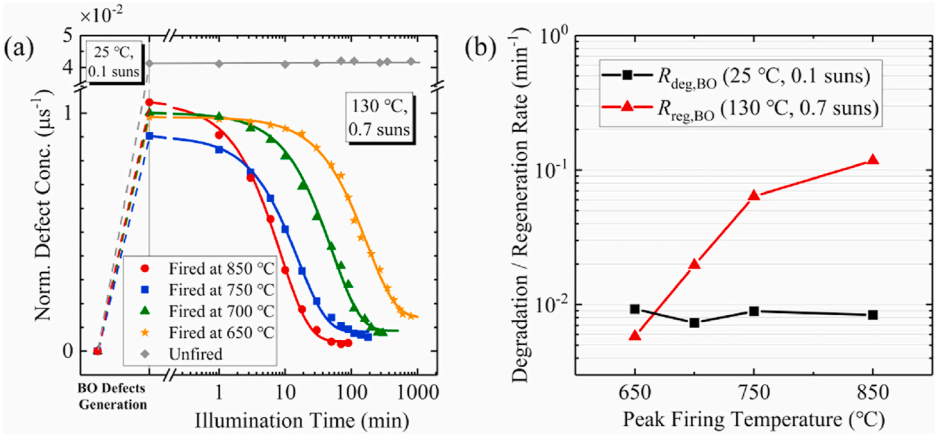

Fig. 3. (a) Changes in normalized defect concentration during generation process (dash lines) and subsequent regeneration process (solid lines) of samples fired (from 650 °C to 850 °C) and unfired. Note that the measurement conditions for defect generation and regeneration are different. (b) The degradation and regeneration rate constants of BO defects as a function of the peak firing temperature.

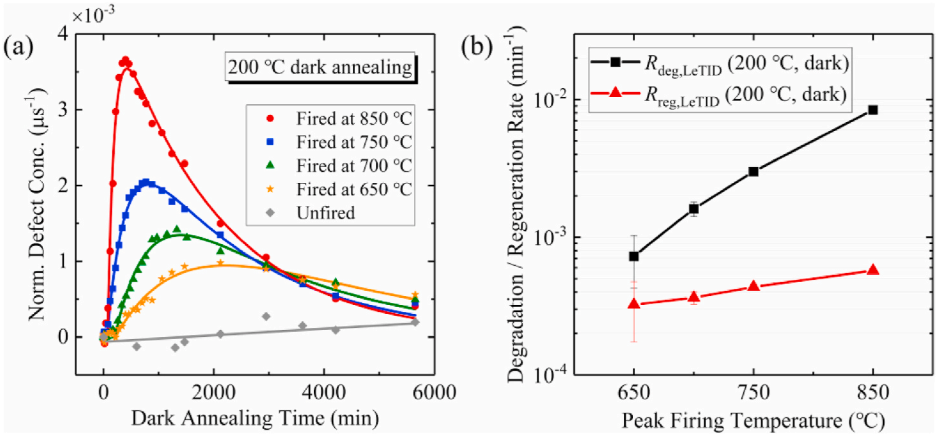

Fig. 4. (a) Normalized defect concentration of samples fired at different temperatures plotted versus the dark annealing time at 200 °C. The curves show the fitting result of Eq. (4). (b) The degradation and regeneration rate constants of LeTID-related defects as a function of the peak firing temperature under dark annealing condition at 200 °C.

$_{LeTID}$ rises mildly. Although our fitting function is simplified, compared to those in previous studies [28], the unambiguous correlation shows that both degradation and regeneration rates are modulated by firing temperature.

Furthermore, we compared the extents of BO-LID and LeTID for the samples fired at different temperatures. As can be seen in Fig. 5, a higher peak firing temperature leads to a larger extent of LeTID, whereas such tendency is not found in BO-LID. Interestingly, we noticed that about 75% of the BO defects in samples fired above 650 °C were deactivated, compared to the unfired sample. With regard to this question, two as-fired samples were subjected to a prolonged dark annealing at 260 °C for 5 h, which is sufficient to destabilize the regenerated BO defects [22,29]. The result shows that with an additional dark annealing process, the subsequently generated BO defect concentration reaches a similar value to unfired samples, supporting our speculation that a large proportion of BO defects has been deactivated by hydrogen during the firing process. The lifetime variations in these experiments are summarized in Table 1, to be compared with related samples. Similar observations were previously reported by Kim et al. [30] and Nampalli et al. [31], pointing out

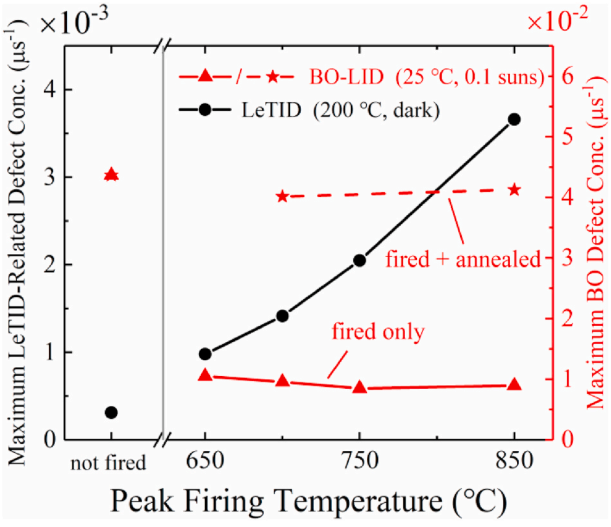

Fig. 5. Maximum defect concentration as a function of peak firing temperature for LeTID-related defects (black) and BO defects (red). Samples with an additional annealing step (red stars) show a similar extent of degradation as the unfired sample. Note that two y-axis scales are different. (For interpretation of the references to colour in this figure legend, the reader is referred to the Web version of this article.)

Table 1
List of samples with different process flows. τ_0 denotes the lifetime after firing. τ_{ann} denotes the lifetime after prolonged dark annealing (if applicable). τ_{deg} denotes the lifetime after degradation. And $N_{t,BO}$ denotes the corresponding normalized BO defect concentration. For samples subjected to prolonged dark annealing at 260 °C for 5 h, the $N_{t,BO}$ is calculated by $1/\tau_{deg} - 1/\tau_{ann}$. The lifetime measurements were carried out at 25 ± 1 °C with a fixed injection level at $\Delta n = 1.5 \times 10^{15}$ cm^{-3}.

Process flow	τ_0 (μs)	τ_{ann} (μs)	τ_{deg} (μs)	$N_{t,BO}$ (μs^{-1})
Not fired	91.4	–	18.8	4.2×10^{-2}
700 °C firing	126.4	–	56.3	1.0×10^{-2}
850 °C firing	148.7	–	63.8	0.9×10^{-2}
700 °C firing + annealing	115.5	117.3	20.5	4.0×10^{-2}
850 °C firing + annealing	147.1	151.0	20.9	4.1×10^{-2}

the firing process can reduce the BO defect concentration.

Even though a large proportion of BO defects in as-fired samples are deactivated, we find that the normalized BO defects concentration is about 1×10^{-2} μs^{-1}, while the value for LeTID-related defects is in the range of 1×10^{-3} μs^{-1} to 4×10^{-3} μs^{-1}, depending on the peak firing temperature. Thus, we suggest that BO-LID may be the dominant degradation mechanism in our Cz-Si samples. Note that this conclusion is specific to the samples in this study, since the degradation extent is affected by many factors. For example, in boron-doped silicon, the maximum defect concentration of BO defects is proportional to the boron concentration and to the square of the oxygen concentration [4].

3.2. The evolution of hydrogen concentration during dark annealing

Based on the hypothesis that the regeneration rate constant of BO defects $R_{reg,BO}$ depends on the hydrogen concentration, we performed BO-LID measurements on the samples subjected to dark annealing with different durations, in order to figure out the evolution of hydrogen concentration during dark annealing. To implement this conception, the samples fired at 850 °C with a lifetime of approximately 150 ± 20 μs were first treated in the dark at 200 °C for different durations, as shown in Fig. 6(a). Three samples were marked as A, B and C, corresponding to the as-fired, degraded and regenerated state of LeTID, respectively. Since the regeneration process was not complete in the sample C, another sample D underwent additional dark annealing at 260 °C for 5 h to reach fully regeneration state. Subsequently, these samples were subjected to BO-LID measurement in order to extract the $R_{reg,BO}$ value, as presented in Fig. 6(b). It shows that increasing the dark annealing duration in the pre-treatment leads to a rising of BO defects concentration. Similar findings have been explained in Section 3.1, as the dark

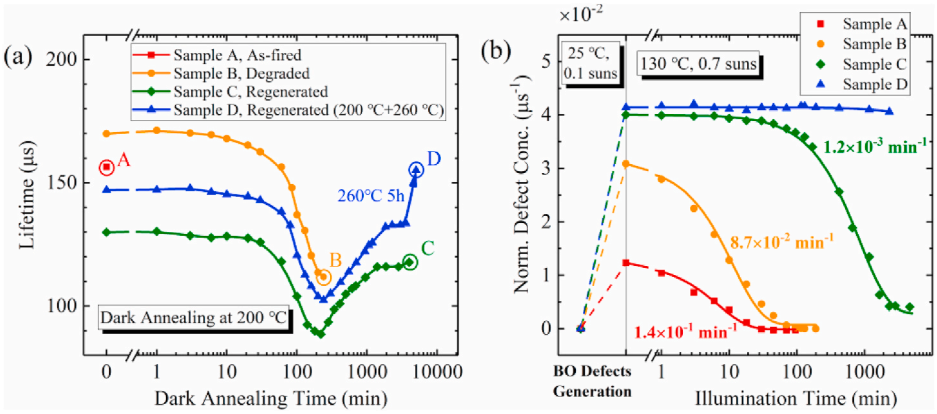

Fig. 6. (a) The effective lifetime as a function of dark annealing time at 200 °C. The treatments were terminated at different states, awaiting the subsequent process. (b) Changes in normalized defect concentration after a complete generation process (dash lines) and then as a function of time under illumination at 130 °C and 0.7 suns (solid lines). The fitting results of $R_{reg,BO}$ using Eq. (3) are labeled in the figure.

annealing condition could destabilize the regenerated BO defects. Moreover, by increasing the dark annealing duration, the regeneration rate constant of BO defects reduced significantly, as the $R_{reg,BO}$ value of sample C is lower than sample A by two orders of magnitude. Extended dark annealing with a higher temperature at 260 °C for 5 h results in a much smaller $R_{reg,BO} < 1 \times 10^{-5}$ min^{-1}, indicating that the deactivation of BO defects is invalid in Sample D.

Fig. 7 summarizes the difference in regeneration rate constant $R_{reg,BO}$ for samples A to D. In previous studies, it has been found that a few minutes of dark annealing could accelerate the regeneration rate of BO defects [22]. Different from that, by extending the dark annealing duration to hours and tens of hours, we find $R_{reg,BO}$ decreases significantly. Based on the hypothesis that $R_{reg,BO}$ value depends on the hydrogen concentration [21,26,27], it seems that LeTID is accompanied by a decrease in hydrogen concentration. However, a noticeable asymmetric of hydrogen concentration reduction can be found in the degradation and regeneration process (see differences between Sample A, B and C in Fig. 7). Thus, it is inappropriate to attribute hydrogen consumption entirely to its participation in the degradation and regeneration of LeTID. Instead, we propose hydrogen also participates in LeTID-irrelevant reactions, which consume hydrogen slowly with a time scale of hours in this case. Based on this speculation, a hydrogen-related model with the reversible reaction is presented later in Section 4.2, in order to illustrate the probable relation between LeTID and the reduction of hydrogen concentration.

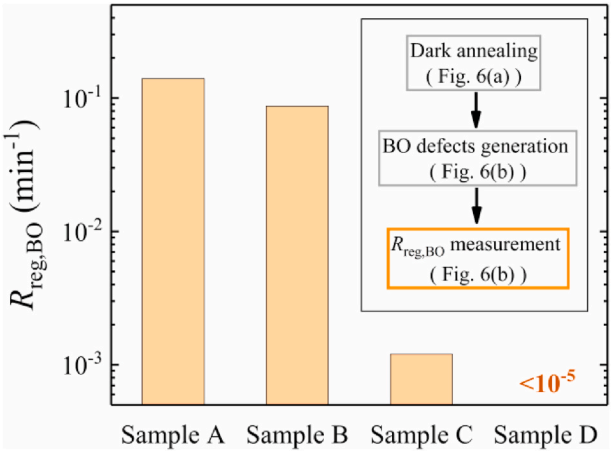

Fig. 7. The extracted regeneration rate constants of BO defects for samples A to D. The inset shows the required experiment process for measuring $R_{reg,BO}$.

4. Discussion

4.1. Interpretations of the peak firing temperature dependence

Our results in Section 3.1 show that firing process has multiple effects on LID in boron-doped Cz-Si. For BO-LID, it has been demonstrated that the regeneration rate can be sped up by higher hydrogen concentration [21,26,27]. In the model proposed by Wilking et al. [22], BO defects are passivated by uncharged H^0 atoms, which dissociated from impurities they were bonding to, e.g., B–H pairs under regeneration condition. This explains our results that the regeneration rate constant accelerates as peak firing temperature rises, since samples q uenched from higher temperature have a larger concentration of B–H pairs [32]. Therefore, we suggest that a higher firing temperature is beneficial to increase the hydrogen concentration and thus passivate BO defects more efficiently.

As for LeTID, several studies have confirmed that the degradation extent increases with the augmentation of peak firing temperature [17,18]. Moreover, based on the fitting results in Fig. 4, we find that higher firing temperatures also raise the degradation and regeneration rate constants of LeTID. As far as the firing dependence is concerned, one may speculate a similar interpretation to that of BO regeneration: mobile H atoms escaped from B–H pairs are the cause of LeTID. This concept has been proposed by several authors [15,28]. Since hydrogen itself seems to be recombination-inactive, complexes formed by mobile H and a homogeneously distributed defect X are more likely to be the LeTID-related defect. Based on this hypothesis, the concentration of mobile H should be much smaller than X, thus the concentration of product H-X is controlled by mobile H, that is, by peak firing temperature. Additionally, another defect model presented by Schmidt et al. proposed that interstitial metal and hydrogen complexes M_i-H are already formed during fast firing step [19]. Afterwards under illumination or dark annealing, M_i-H complexes dissociate and the isolated M_i is assumed to be highly recombination-active, thus causing the degradation. This model can also explain the firing dependence, as the degradation extent is related to the concentration of M_i-H formed during firing step. On the transitions of LeTID-related defect, more details will be discussed in Section 4.2.

As mentioned above, firing temperature dependence of both BO-LID and LeTID can be explained by the variation of mobile hydrogen concentration, although exactly how hydrogen participates in those reactions remains to be explored. Based on the results, we suggest that high hydrogen concentration in silicon bulk leads to large extent and rapid degradation of LeTID, while low hydrogen concentration cannot afford an efficient passivation of BO defects. Therefore, more attention should be paid when introducing thermal treatment on p-type Cz-Si

solar cells, since the hydrogen concentration and bonding state change considerably after thermal treatment.

4.2. Hydrogen-related defect model of LeTID

Although the measurement in Fig. 6 is rather complicated, some features can be unambiguously drawn: (1) under dark annealing condition, LeTID-related defect concentration is firstly increased and then reduced, (2) in timescale of hours, during dark annealing, the concentration of mobile hydrogen is reduced over time. Therefore, we propose a hydrogen-related LeTID model to interpret our findings, which contains a simple reversible reaction:

$$H + X \rightleftharpoons HX \tag{5}$$

where H is mobile hydrogen, X is a homogeneously distributed unknown defect. Here, we assume that X is recombination-inactive and already existent after the firing process. Under illumination at elevated temperature or dark annealing, these two precursors could form highly recombination-active HX complex, which leads to a lifetime degradation.

For the fired sample, a large concentration of hydrogen is trapped in silicon bulk and forms B–H pairs or H_2 dimers [33], both of which could further release mobile hydrogen under dark annealing [33,34]. Thus, in the early duration of dark annealing (e.g. fist 300 min in Fig. 6(a)), the reactant mobile hydrogen is abundant, leading to a rapid forward reaction to form HX complexes until equilibrium is reached, which is considered to be the degradation process of LeTID. On the contrary, for the unfired sample, HX complexes cannot be formed since hydrogen is not present in silicon bulk (thus no LeTID is observed).

After reaching the maximum degradation point, an equilibrium is established between the mobile hydrogen and HX complexes. However, apart from the formation of HX complexes, the mobile hydrogen also forms stable H_{2C} dimers or out-diffuse to the surface [23], which are considered as irreversible reactions and will consume large amounts of mobile hydrogen throughout LeTID process. As the concentration of reactant mobile hydrogen continuously decreases, the equilibrium of the reaction shifts to the left, requiring more HX complexes dissociation. Hence, the concentration of recombination-active HX complexes is also reduced accordingly during extended dark annealing (e.g. after 300 min in Fig. 6(a)), resulting in a lifetime recovery. When the mobile hydrogen is completely depleted in the bulk, the HX complexes run out correspondingly.

The evolution of HX complex concentration can also be described by the following differential equation:

$$d[HX]/dt = R_g[H][X] - R_d[HX] \tag{6}$$

where R_g and R_d are the generation and dissociation rate constants, respectively. Clearly, the d [HX]/dt term depends highly on the mobile hydrogen concentration [H]. Although it is complicated to present the d [H]/dt in equation, we can estimate that [H] significantly reduced during the long-term dark annealing, based on the result of experiment in Section 3.2. According to Eq. (6), after reaching equilibrium (d [HX]/dt = 0), the decrease of [H] means d [HX]/dt < 0, equivalent to the dissociation of HX complexes. Therefore, the correlation between the regeneration process of LeTID and the decrease of [H] is established.

In order to solve Eq. (6), two assumptions are made: (I) mobile hydrogen concentration decreases exponentially with time, and (II) concentration of X defect is much larger than the concentrations of H and HX. Hence, [H] and [X] can be described with following functions:

$$[H] = N_{H,total} \exp(-R_c t) - [HX] \tag{7}$$

$$[X] = N_X \tag{8}$$

where R_c is the consumption rate constant of hydrogen, $N_{H,total}$ is the initial concentration of mobile hydrogen, N_X is the concentration of X defect. The solution of Eqs. (6)–(8) gives [HX] of:

$$[HX] = \frac{N_{H,total} N_X R_g}{R_c - N_X R_g - R_d}\left(\exp\left(-N_X R_g t - R_d t\right) - \exp(-R_c t)\right) \tag{9}$$

Interestingly, this function is similar with Eq. (4) in terms of form, as both are double exponential functions. Comparing Eq. (4) with Eq. (9), it seems that the measured regeneration rate $R_{reg,\ LeTID}$ is equivalent to the consumption rate of mobile hydrogen R_c, which is in line with our assumption. The degradation rate seems to depend on N_X, R_g and R_d. However, this inference is not rigorous enough, for the calculation neglects the release process of mobile hydrogen, which may probably dominate the degradation rate of LeTID. Furthermore, Eq. (9) cannot fully explain the firing temperature dependence of LeTID kinetics, as shown in Fig. 4. Indeed, an exponential function seems a bit oversimplifying for the consumption process of mobile hydrogen, and may lose sight of its dependence on the total hydrogen concentration, which is modulated by firing temperature. In the further research, a more rigorous derivation and calculation is needed to refine the proposed defect model.

There have been several literatures discussing hydrogen-related LeTID models [15,28], which share some similarities with our model presented above. Sio et al. [35] also suggested that dark annealing would cause another individual reaction apart from the LeTID degradation, which could reduce the amount of hydrogen in silicon bulk. However, different from their three-state model, we find it is reasonable to explain LeTID with only one reversible reaction, that is, the generation and dissociation of HX complexes. In addition, we interpret the regeneration process of LeTID in a new hypothesis, that is, the gradually reducing hydrogen concentration would cause the dissociation of recombination-active HX complexes, hence a rise in the lifetime.

Moreover, this model is based on the behavior of LeTID observed during dark annealing condition, under which reactions are thermally activated. For standard LeTID condition, the defects are activated by excess carrier injection through illumination or forward-biasing. Despite the different triggering methods, the formed recombination-active defects have been proved to have a similar capture cross-section ratio value k [11,36], indicating that they are likely the same defect. Additionally, the activation energy of degradation process is determined as ~1.1 eV for dark annealing condition [36], and ~0.9 eV for illumination condition [37]. This slight difference can be explained by the different source of mobile hydrogen, as carriers may enhance the dissociation of B–H pairs or H_2 dimers [23,34]. Therefore, our model may still be plausible under illumination condition. However, the possibility should be mentioned that the degradation mechanisms are different between dark annealing and carrier injection conditions [38], thus their activation energies are not equal.

Concerning the chemical species of X defect, our findings cannot yield specific clues to identify it. According to the literature, several kinds of metal impurities (e.g. Fe, Co, Ni, Ti) have been considered as candidates for the involvement of LeTID [9,19,39]. Additionally, intrinsic lattice defects such as interstitial silicon atoms or vacancies should also be taken into account, since LeTID is also observed in floatzone (Fz) silicon [40].

5. Conclusions

In summary, the behavior of LID in boron-doped Cz-Si wafers with PERC structure have been investigated. By adopting different measurement conditions, we find that both BO-LID and LeTID can cause severe degradation. Furthermore, the impact of peak firing temperature on LID is investigated. The results show that the rate constants $R_{reg,BO}$, $R_{deg,\ LeTID}$ and $R_{reg,\ LeTID}$ as well as the extent of LeTID are dependent on the peak firing temperature. These dependences can be interpreted by the variation of hydrogen concentration, which further indicates that high hydrogen concentration leads to a larger extent and rapid degradation of

LeTID, while low hydrogen concentration cannot afford an efficient passivation of BO defects. Thus, modulating hydrogen concentration may be crucial for eliminating LID in Cz-Si solar cells.

Moreover, extending the duration of dark annealing pre-treatment decelerates the subsequent regeneration rate of BO defects. This result implies that, under dark annealing, the evolution of LeTID is accompanied by a decrease in the mobile hydrogen concentration. Based on this, a hydrogen-related model with the reversible reaction is proposed to describe the behavior of LeTID under dark annealing. We suggest that the degradation process of LeTID is due to the establishment of equilibrium between the precursor and the recombination-active HX complexes, while the regeneration process is due to the dissociation of HX complexes during the shift of equilibrium towards the reactant side. Note that X could be metal impurities or intrinsic crystal defects, according to the literature.

CRediT authorship contribution statement

Dehang Lin: Conceptualization, Methodology, Writing – original draft. **Zechen Hu:** Methodology. **Qiyuan He:** Formal analysis. **Deren Yang:** Project administration. **Lihui Song:** Methodology, Writing – review & editing. **Xuegong Yu:** Supervision, Funding acquisition.

Declaration of competing interest

The authors declare that they have no known competing financial interests or personal relationships that could have appeared to influence the work reported in this paper.

Acknowledgments

This project is supported by National Natural Science Foundation of China (No. 62025403, 61974129, 61721005), National Key Research and Development Project (2018YFB1500401) and Visiting Scholars Foundation of State Key Laboratory of Silicon Materials (SKL2020-01).

References

[1] A. Blakers, Development of the PERC solar cell, IEEE J. Photovoltaics. 9 (2019) 629–635, https://doi.org/10.1109/jphotov.2019.2899460.
[2] J. Schmidt, A. Cuevas, Electronic properties of light-induced recombination centers in boron-doped Czochralski silicon, J. Appl. Phys. 86 (1999) 3175–3180, https://doi.org/10.1063/1.371186.
[3] K. Bothe, J. Schmidt, Electronically activated boron-oxygen-related recombination centers in crystalline silicon, J. Appl. Phys. 99 (2006) 13701, https://doi.org/10.1063/1.2140584.
[4] K. Bothe, R. Sinton, J. Schmidt, Fundamental boron-oxygen-related carrier lifetime limit in mono- and multicrystalline silicon, Prog. Photovoltaics Res. Appl. 13 (2005) 287–296, https://doi.org/10.1002/pip.586.
[5] A. Herguth, G. Schubert, M. Kaes, G. Hahn, Investigations on the long time behavior of the metastable boron–oxygen complex in crystalline silicon, Prog. Photovoltaics Res. Appl. 16 (2008) 135–140, https://doi.org/10.1002/pip.779.
[6] B. Lim, K. Bothe, J. Schmidt, Deactivation of the boron–oxygen recombination center in silicon by illumination at elevated temperature, Phys. Status Solidi Rapid Res. Lett. 2 (2008) 93–95, https://doi.org/10.1002/pssr.200802009.
[7] K. Ramspeck, S. Zimmermann, H. Nagel, A. Metz, Y. Gassenbauer, B. Brikmann, A. Seidl, Light induced degradation of rear passivated mc-Si solar cells. Proceedings of the 27th European Photovoltaic Solar Energy Conference, 2012, pp. 861–865, https://doi.org/10.4229/27THEUPVSEC2012-2DO.3.4.
[8] F. Fertig, K. Krauß, S. Rein, Light-induced degradation of PECVD aluminium oxide passivated silicon solar cells, Phys. Status Solidi Rapid Res. Lett. 9 (2015) 41–46, https://doi.org/10.1002/pssr.201409424.
[9] K. Nakayashiki, J. Hofstetter, A.E. Morishige, T.-T.A. Li, D.B. Needleman, M. A. Jensen, T. Buonassisi, Engineering solutions and root-cause analysis for light-induced degradation in *p*-type multicrystalline silicon PERC modules, IEEE J. Photovoltaics. 6 (2016) 860–868, https://doi.org/10.1109/jphotov.2016.2556981.
[10] F. Kersten, P. Engelhart, H.-C. Ploigt, A. Stekolnikov, T. Lindner, F. Stenzel, M. Bartzsch, A. Szpeth, K. Petter, J. Heitmann, J.W. Müller, Degradation of multicrystalline silicon solar cells and modules after illumination at elevated temperature, Sol. Energy Mater. Sol. Cells 142 (2015) 83–86, https://doi.org/10.1016/j.solmat.2015.06.015.
[11] D. Chen, M. Kim, B. V Stefani, B.J. Hallam, M.D. Abbott, C.E. Chan, R. Chen, D.N. R. Payne, N. Nampalli, A. Ciesla, T.H. Fung, K. Kim, S.R. Wenham, Evidence of an identical firing-activated carrier-induced defect in monocrystalline and multicrystalline silicon, Sol. Energy Mater. Sol. Cells 172 (2017) 293–300, https://doi.org/10.1016/j.solmat.2017.08.003.
[12] M. Wagner, F. Wolny, M. Hentsche, A. Krause, L. Sylla, F. Kropfgans, M. Ernst, R. Zierer, P. Bönisch, P. Müller, N. Schmidt, V. Osinniy, H.-P. Hartmann, R. Mehnert, H. Neuhaus, Correlation of the LeTID amplitude to the Aluminium bulk concentration and Oxygen precipitation in PERC solar cells, Sol. Energy Mater. Sol. Cells 187 (2018) 176–188, https://doi.org/10.1016/j.solmat.2018.06.009.
[13] F. Fertig, R. Lantzsch, A. Mohr, M. Schaper, M. Bartzsch, D. Wissen, F. Kersten, A. Mette, S. Peters, A. Eidner, J. Cieslak, K. Duncker, M. Junghänel, E. Jarzembowski, M. Kauert, B. Faulwetter-Quandt, D. Meißner, B. Reiche, S. Geißler, S. Hörnlein, C. Klenke, L. Niebergall, A. Schönmann, A. Weihrauch, F. Stenzel, A. Hofmann, T. Rudolph, A. Schwabedissen, M. Gundermann, M. Fischer, J.W. Müller, D.J.W. Jeong, Mass production of p-type Cz silicon solar cells approaching average stable conversion efficiencies of 22 %, Energy Procedia 124 (2017) 338–345, https://doi.org/10.1016/j.egypro.2017.09.308.
[14] D. Chen, P.G. Hamer, M. Kim, T.H. Fung, G. Bourret-Sicotte, S. Liu, C.E. Chan, A. Ciesla, R. Chen, M.D. Abbott, B.J. Hallam, S.R. Wenham, Hydrogen induced degradation: a possible mechanism for light- and elevated temperature- induced degradation in n-type silicon, Sol. Energy Mater. Sol. Cells 185 (2018) 174–182, https://doi.org/10.1016/j.solmat.2018.05.034.
[15] S. Liu, D. Payne, C. Vargas Castrillon, D. Chen, M. Kim, C. Sen, U. Varshney, Z. Hameiri, C. Chan, M. Abbott, S. Wenham, Impact of dark annealing on the kinetics of light- and elevated-temperature-induced degradation, IEEE J. Photovoltaics 8 (2018) 1494–1502, https://doi.org/10.1109/jphotov.2018.2866325.
[16] F. Kersten, J. Heitmann, J.W. Müller, Influence of Al2O3 and SiNx passivation layers on LeTID, Energy Procedia 92 (2016) 828–832, https://doi.org/10.1016/j.egypro.2016.07.079.
[17] C.E. Chan, D.N.R. Payne, B.J. Hallam, M.D. Abbott, T.H. Fung, A.M. Wenham, B. S. Tjahjono, S.R. Wenham, Rapid stabilization of high-performance multicrystalline P-type silicon PERC cells, IEEE J. Photovoltaics. 6 (2016) 1473–1479, https://doi.org/10.1109/jphotov.2016.2606704.
[18] D. Bredemeier, D. Walter, S. Herlufsen, J. Schmidt, Understanding the light-induced lifetime degradation and regeneration in multicrystalline silicon, Energy Procedia 92 (2016) 773–778, https://doi.org/10.1016/j.egypro.2016.07.060.
[19] J. Schmidt, D. Bredemeier, D.C. Walter, On the defect physics behind light and elevated temperature-induced degradation (LeTID) of multicrystalline silicon solar cells, IEEE J. Photovoltaics. 9 (2019) 1497–1503, https://doi.org/10.1109/jphotov.2019.2937223.
[20] C. Vargas, K. Kim, G. Coletti, D. Payne, C. Chan, S. Wenham, Z. Hameiri, Carrier-induced degradation in multicrystalline silicon: dependence on the silicon nitride passivation layer and hydrogen released during firing, IEEE J. Photovoltaics. 8 (2018) 413–420, https://doi.org/10.1109/jphotov.2017.2783851.
[21] S. Wilking, A. Herguth, G. Hahn, Influence of hydrogen on the regeneration of boron-oxygen related defects in crystalline silicon, J. Appl. Phys. 113 (2013) 194503, https://doi.org/10.1063/1.4804310.
[22] S. Wilking, C. Beckh, S. Ebert, A. Herguth, G. Hahn, Influence of bound hydrogen states on BO-regeneration kinetics and consequences for high-speed regeneration processes, Sol. Energy Mater. Sol. Cells 131 (2014) 2–8, https://doi.org/10.1016/j.solmat.2014.06.027.
[23] V. V Voronkov, R. Falster, Formation, dissociation, and diffusion of various hydrogen dimers in silicon, Phys. Status Solidi 254 (2017) 1600779, https://doi.org/10.1002/pssb.201600779.
[24] R.A. Sinton, A. Cuevas, Contactless determination of current–voltage characteristics and minority-carrier lifetimes in semiconductors from quasi-steady-state photoconductance data, Appl. Phys. Lett. 69 (1996) 2510–2512, https://doi.org/10.1063/1.117723.
[25] B. Lim, V. V Voronkov, R. Falster, K. Bothe, J. Schmidt, Lifetime recovery in p-type Czochralski silicon due to the reconfiguration of boron–oxygen complexes via a hole-emitting process, Appl. Phys. Lett. 98 (2011) 162104, https://doi.org/10.1063/1.3581215.
[26] G. Krugel, W. Wolke, J. Geilker, S. Rein, R. Preu, Impact of hydrogen concentration on the regeneration of light induced degradation, Energy Procedia 8 (2011) 47–51, https://doi.org/10.1016/j.egypro.2011.06.100.
[27] G. Hahn, S. Wilking, A. Herguth, BO-related defects: overcoming bulk lifetime degradation in crystalline Si by regeneration, Solid State Phenom. 242 (2015) 80–89. https://doi.org/10.4028/www.scientific.net/SSP.242.80.
[28] T.H. Fung, M. Kim, D. Chen, C.E. Chan, B.J. Hallam, R. Chen, D.N.R. Payne, A. Ciesla, S.R. Wenham, M.D. Abbott, A four-state kinetic model for the carrier-induced degradation in multicrystalline silicon: introducing the reservoir state, Sol. Energy Mater. Sol. Cells 184 (2018) 48–56, https://doi.org/10.1016/j.solmat.2018.04.024.
[29] A. Herguth, G. Hahn, Kinetics of the boron-oxygen related defect in theory and experiment, J. Appl. Phys. 108 (2010) 114509, https://doi.org/10.1063/1.3517155.
[30] M. Kim, S. Wenham, V. Unsur, A. Ebong, B. Hallam, Impact of rapid firing thermal processes on meta-stable defects: preformation of the LeTID and the suppression of B-O defects, in: IEEE 7th World Conf. Photovolt. Energy Convers. (A Jt. Conf. 45th IEEE PVSC, 28th PVSEC 34th EU PVSEC), 2018, pp. 341–346, https://doi.org/10.1109/PVSC.2018.8547666, 2018.
[31] N. Nampalli, H. Li, M. Kim, B. Stefani, S. Wenham, B. Hallam, M. Abbott, Multiple pathways for permanent deactivation of boron-oxygen defects in p-type silicon, Sol. Energy Mater. Sol. Cells 173 (2017) 12–17, https://doi.org/10.1016/j.solmat.2017.06.041.

[32] M.J. Binns, R.C. Newman, S.A. McQuaid, E.C. Lightowlers, Hydrogen solubility and defects in silicon, Mater. Sci. Forum 143–147 (1993) 861–866. https://doi.org/10.4028/www.scientific.net/MSF.143-147.861.
[33] R.E. Pritchard, J.H. Tucker, R.C. Newman, E.C. Lightowlers, Hydrogen molecules in boron-doped crystalline silicon, Semicond. Sci. Technol. 14 (1999) 77–80, https://doi.org/10.1088/0268-1242/14/1/011.
[34] T. Zundel, J. Weber, Boron reactivation kinetics in hydrogenated silicon after annealing in the dark or under illumination, Phys. Rev. B 43 (1991) 4361–4372, https://doi.org/10.1103/PhysRevB.43.4361.
[35] H.C. Sio, H. Wang, Q. Wang, C. Sun, W. Chen, H. Jin, D. Macdonald, Light and elevated temperature induced degradation in p-type and n-type cast-grown multicrystalline and mono-like silicon, Sol. Energy Mater. Sol. Cells 182 (2018) 98–104, https://doi.org/10.1016/j.solmat.2018.03.002.
[36] C. Vargas, G. Coletti, C. Chan, D. Payne, Z. Hameiri, On the impact of dark annealing and room temperature illumination on p-type multicrystalline silicon wafers, Sol. Energy Mater. Sol. Cells 189 (2019) 166–174, https://doi.org/10.1016/j.solmat.2018.09.018.
[37] D. Bredemeier, D. Walter, J. Schmidt, Light-induced lifetime degradation in high-performance multicrystalline silicon: detailed kinetics of the defect activation, Sol. Energy Mater. Sol. Cells 173 (2017) 2–5, https://doi.org/10.1016/j.solmat.2017.08.007.
[38] T. Luka, M. Turek, C. Hagendorf, Defect formation under high temperature dark-annealing compared to elevated temperature light soaking, Sol. Energy Mater. Sol. Cells 187 (2018) 194–198, https://doi.org/10.1016/j.solmat.2018.06.043.
[39] D. Bredemeier, D.C. Walter, J. Schmidt, Possible candidates for impurities in mc-Si wafers responsible for light-induced lifetime degradation and regeneration, Sol. RRL. 2 (2018) 1700159, https://doi.org/10.1002/solr.201700159.
[40] T. Niewelt, F. Schindler, W. Kwapil, R. Eberle, J. Schön, M.C. Schubert, Understanding the light-induced degradation at elevated temperatures: similarities between multicrystalline and floatzone p-type silicon, Prog. Photovoltaics Res. Appl. 26 (2018) 533–542, https://doi.org/10.1002/pip.2954.